LHC Beam Loss Monitor System Design

B. Dehning*, G. Ferioli*, W. Friesenbichler*, E. Gschwendtner* and J. Koopman*

*CERN, CH1211 Geneva 23, Switzerland

Abstract. At the LHC a beam loss system will be installed for continuous surveillance of particle losses. The system is designed to prevent hardware destructions, to avoid magnet coil quenches and to provide quantitative loss values. Over 3000 ionization chambers will be used to initiate the beam abort if the loss rates exceed the quench levels. The time and beam energy dependent quench levels require the acquisition of chamber currents in the range from 50 pA to 0.5 mA and an update of the values every 89 μs. The acquisition and control electronics will consist of a front end electronics near (< 400 m) to the ionization chambers and a threshold controller in the surface buildings. The front end will include a charge balance converter, a counter and multiplexer part. The charge balance converter is most suiteable to cover the large dynamic range. The introduced error is smaller than few % in the required dynamic range. Six channels will be transmitted over one cable of up to 3 km length. The threshold controller will issue warnings and dump signals depending on the beam energy and the loss durations.

INTRODUCTION

At the nominal energy of 7 TeV each beam in the LHC stores energy of up to 0.35 GJ. The loss of only a fraction (10^{-8}) of the beam can have a severe impact on the smooth machine operation. Therefore the beam loss detection system must fulfil several requirements, first: Protection: The magnets and other equipments must be protected from damage due to beam losses. Second: Prevention: The super conducting coils of the magnets could be come normal conducting by heat depostion from lost particles. In both cases beam dumps are initiated before a dammage or quench will occur. Thired: Serve as a beam diagnostic tool.

For protection and prevention the beam loss monitors trigger the beam dump via the beam interlock system, whenever they detect beam losses above a certain limit. The quench levels of the super-conducting magnets define this limit.

Detection of shower particles outside the cryostat or near to the collimators will be used to determine the coil temperature increase due to particle losses. The relation between loss rate and temperature increase (quench levels) is based on shower simulation and heat transfer considerations [1]. The expected particle flux outside the cryostat is as well based on shower simulation.

CP648, *Beam Instrumentation Workshop 2002: Tenth Workshop*, edited by G. A. Smith and T. Russo

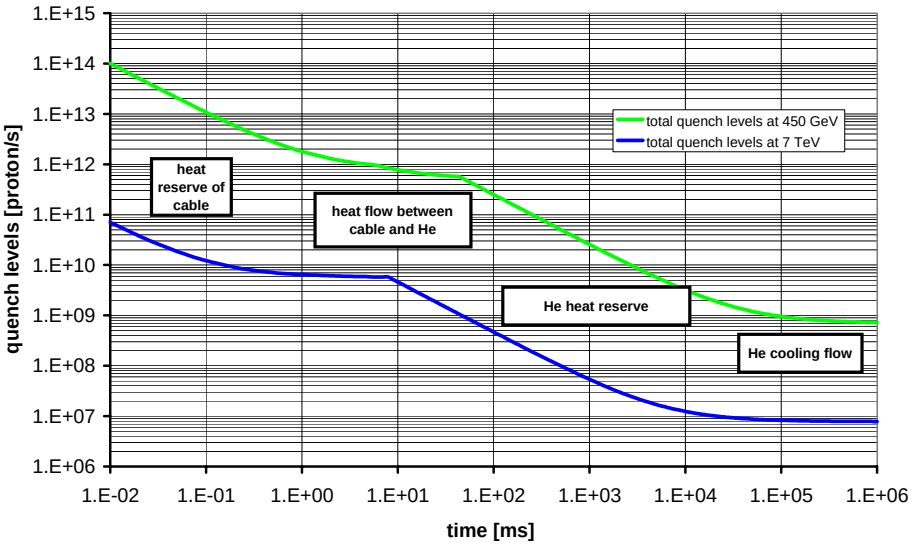

FIGURE 1. The bending magnet quench levels as function of the loss duration for two different energies.

QUENCH LEVELS

The coils of the magnets can quench if a local energy deposition due to beam particle losses increases the coil temperature to a value were the conductor changes from the super-conducting to normal conducting state [1, 2]. In addition to the energy dependence of the quench levels (see Fig. 1), a strong dependence on the duration of the loss is observed. At 450 GeV the quench limit rate is 1 10^{13} protons/s corresponding 0.9 10^{9} protons for a loss duration of 1 turn (89 μs) and the state state rate (t > 100 s) is 7 10^{8} protons/s. At 7 TeV the magnet quench rate is 1 10^{10} protons/s corresponding to 0.9 10^{5} protons per turn and the state state rate (t > 50 s) is 8 10^{6} protons/s.

The thermal conductivity of the surrounding helium flow determines the maximum loss rate at long time intervals. At short time intervals, the heat reserve of the cables, as well as the heat flow between the superconducting cables and the helium, tolerates much higher loss rates. The heat reserve of the helium determines the quench levels at intermediate time scales.

BEAM LOSS PARTICLE DETECTION

At the positions, where most of the beam losses are expected, simulations of the particle fluences outside the cryostat induced by lost protons at the aperture have been performed with the Monte Carlo Code Geant 3.21. The geometry used in this simulation corresponds to the dispersion suppressor. Calculations for the arc have already been presented in [2]. The simulated shower particles produced by lost protons are counted in

two detectors placed all along the cryostat on both sides. Also the energy deposition in these elements is calculated. Figure 2 gives a typical example of detector signals caused

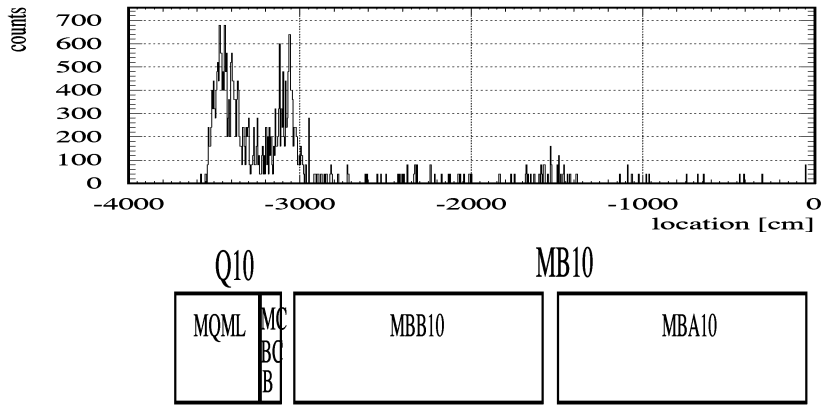

FIGURE 2. Simulated detector signals of shower particles, caused by a point like loss in the middle of the quadrupole magnet MQML.

by the shower particles, which are induced by point like losses of the beam in the middle of the quadrupole MQML (β-function maximum). The shower maximum is about 1 m after the beam loss location. The shower width is 0.7 m. For one lost proton of 7 TeV 110^{-2} charged particles/proton/cm^2 are observed. The second shower maximum is due to the gap between the quadrupole (MQML) and the dipole (MBB). The signals in the detectors on the opposite side of the cryostat are reduced in amplitude and the beam loss maxima from beam 1 and beam 2 are separated between 1 and 2 m [3]. Positioning beam loss monitors at the shower maxima locations fulfils the requirements for the distinction between the two beams and for localising the beam losses. It is foreseen to place three detectors on either side of the cryostat 3 at the optimal position for the observation of beam losses located in the middle of the quadrupole magnet and located at the transitions between the quadrupole magnet and the bending magnets.

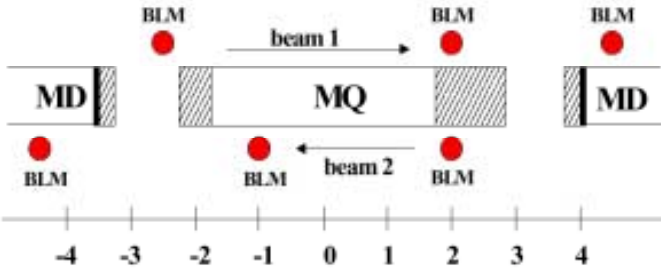

FIGURE 3. Location of the beam loss detectors near to the quadrupole magnets MQ.

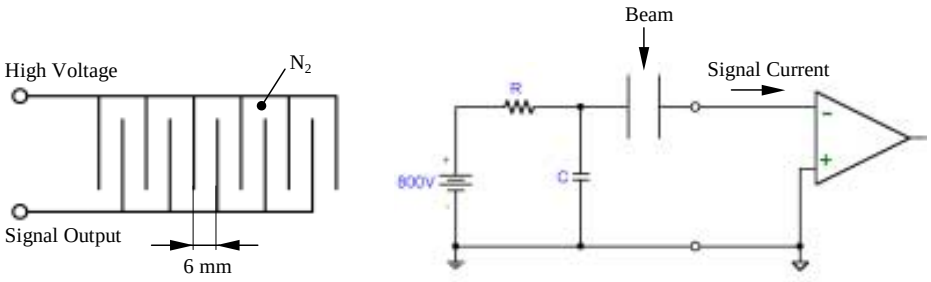

FIGURE 4. Left: Schematic structure of the baseline ionisation chamber. Right: Principle circuit diagram for the frontend electronic circuit.

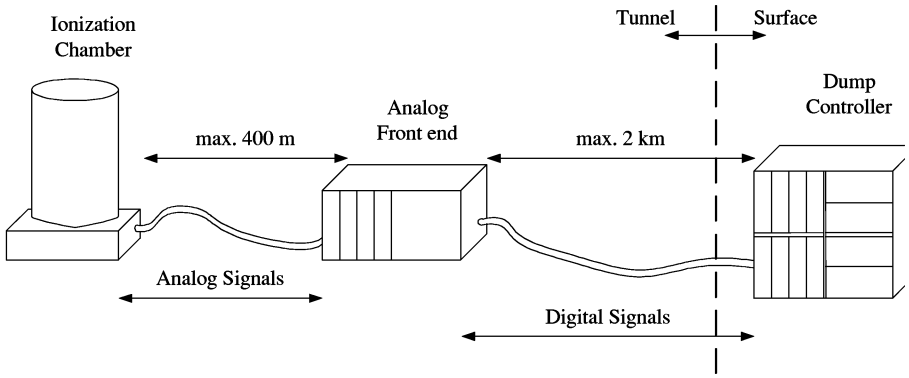

FIGURE 5. Schematic of the beam loss monitor readout chain.

BEAM LOSS DETECTORS

Ionisation chambers will be used as beam loss monitors. The baseline layout is a N_2 filled cylinder with a surface of 80 cm^2, a length of 19 cm and operated with a bias voltage of V = 800 - 1800 V (see fig. 4). The chamber electrodes consist of 31 parallel plates. All the odd and even plates are connected together to increase the electrical field volume, which has a strenght of up to 3 kV/cm. To stabilize the high voltage an low pass filter (R = 1 MΩ and C = 0.5μF) is mounted on the chamber feed throughs.

STRUCTURE OF THE BEAM LOSS MONITOR READOUT CHAIN

The first evaluation of this signal is done by the analog front end. Due to radiation exposure in the accelerator tunnel, the cable length between the chamber and the front end can vary between several meters in the arcs of the tunnel, and up to 400 m in the straight sections (see fig. 5). The increased radiation load in the tunnel (up to 10 Gray

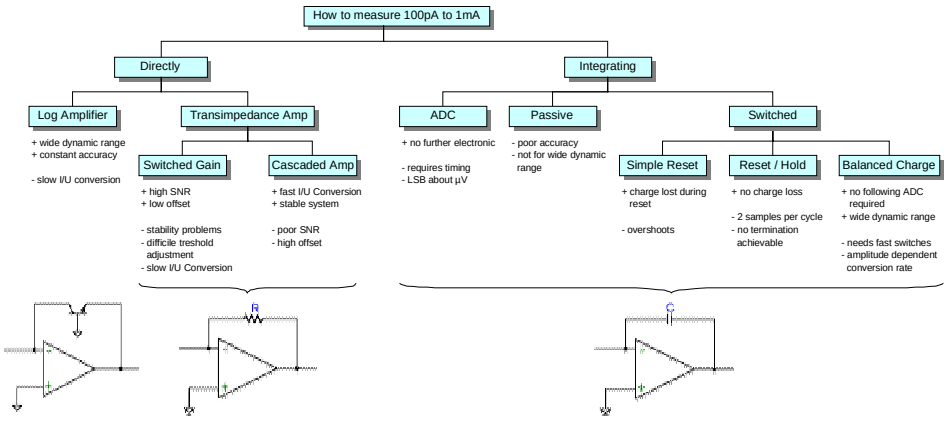

FIGURE 6. Overview of the applicable principles to measure electrical currents.

per year are expected) necessitates a simple and robust design of the front end circuitry. The final evaluation and the beam dump decision is made by the threshold controller, which is located in a surface building. The threshold controllers are located at eight locations where they are connection to the beam abort system. The cable lenght between the frontend electronic and the threshold controllers varriers between 1.8 and 2 km The threshold controller itself calculates the beam losses for different loss durations and beam energies and compares them with the appropriate treshold values. A warning or beam dump signal is generated if the tresholds are exceeded.

FRONT END ELECTRONIC DESIGN

The quench levels are varying between 600 pA and 500 μA. To ensure high sensitivity at low losses, the dynamic range must be extended at least one order of magnitude from 600 pA down to 60 pA. Thus the lower limit was set to 50 pA, which results in a dynamic range of 140 dB.

The integrated loss rate has to be acquired in an interval between 89 μs and 100. The minimum time limit is given by the fastest beam dump possibility after one revolution (89 μs) and the longest interval is set by the temperature measurement system of the He of the magnets to 100 s. Simulation studies revealed [1] that the quench level prediction is accurate to $\pm$50 %. Consequently, the maximum allowable error of the readout electronics was set to $\pm$10 %.

The usage of the ionization chamber leads to the measurement of a particle loss rate equivalent electric current. Several design considerations to acquire this current have been made [4]. Figure 6 shows an overview of the different methods that have been taken into account.

Direct monitoring techniques provide an output signal that is proportional to the input current. A transimpedance amplifier, e.g., transforms the input current into a proportional voltage. The output voltage can be sampled with an ADC at the required

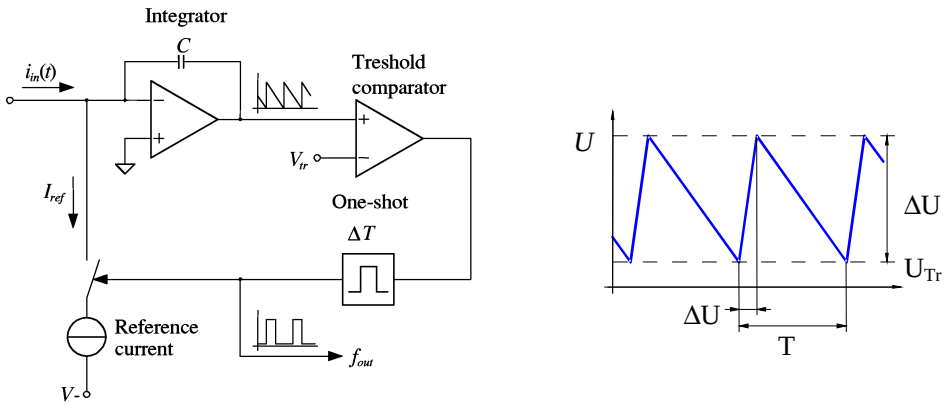

FIGURE 7. Left: Circuit diagram of the current to frequency converter. Right: Output voltage of the operational amplifier versus time applying a constant input current.

frequency, which is determined by the evaluation time of the particle loss rate. It is not possible to achieve with this method a dynamic range of more than approximately 60 dB without introducing large errors. Thus several gain stages have to be incorporated, which have some other features (see pros and cons indicated at the figure: 6).

Integrating techniques compared to direct monitoring provide only average loss rates, but offers unique properties in terms of dynamic range and the signal to noise ratio. The most simple way to realize such a circuit would be an ADC that offers a high dynamic range. Several components, especially for audio applications, have been found but none offered a sufficient low input current. The switched integrator is a widely used circuit to measure small currents. An electric current charges the feedback capacitor of an operational amplifier and the output voltage is equal to the integral of the current over time. However, the dynamic range is only 60 dB. This range can be extended, if a certain treshold voltage is introduced. If the output voltage reaches the treshold within the time interval, the integrator will be reset. At the end of the integration interval, the actual output voltage is sampled as before, but also the number of reset actions within the interval are taken into account. As long as the reset time is much shorter than the integration time, the introduced error can be neglected.

The current to frequency converter functional principle (CFC) is shown in figure 7. It consists of an integrator, whose capacitor is charged by the signal current and discharged by a fixed reference current. The concept of a CFC was successfully improved and used by H. Reeg [5, 6]. The authors investigations are based on the work of E. G. Shapiro [7].

Figure 7, right depicts a typical analog output voltage of the CFC with a constant input current that is almost at the maximum value of the operating range. If the output voltage ramps negative and reaches the treshold voltage U_{Tr}, the one-shot switches the reference current source I_{ref} to the summing node for a fixed time interval ΔT. As the reference current has the opposite polarity and is larger as the signal current, the integrator output voltage is increasing. Later I_{ref} is disconnected, the output ramps again down until it reaches the threshold potential. Assuming an ideal operational amplifier, with no input

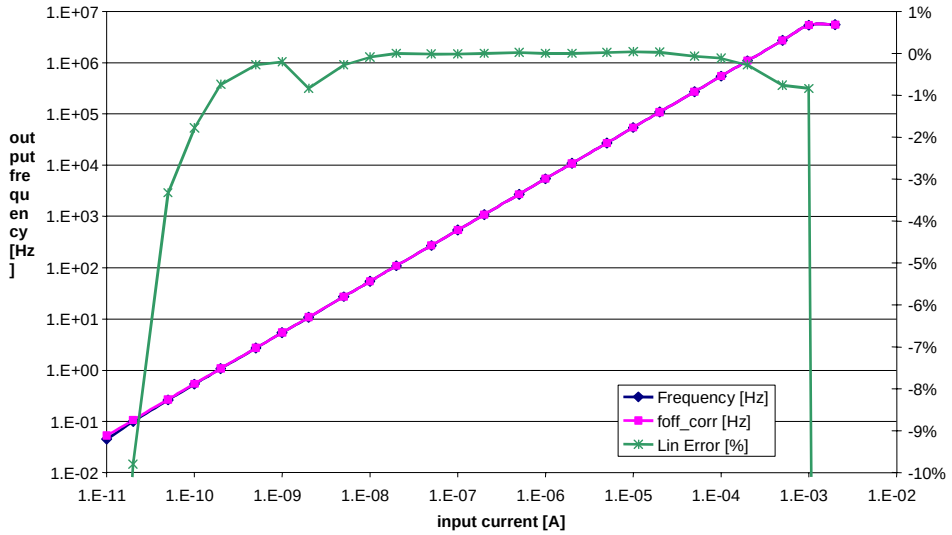

FIGURE 8. CFC output frequency and linearity error versus input current for a maximum current of 2 mA.

current and no offset voltage, a fixed charge $Q_{ref} = I_{ref} \cdot \Delta T$ is extracted from the summing node at the operational amplifier during the reset period ΔT. This charge is equal to the the total signal input charge during the period T. Because the signal charge and the capacitor charge are equal to $Q_{ref} = I_{ref} \cdot \Delta T$ during the time ΔT and since the accumulated charge of the capacitor during the period ΔT and $T - \Delta T$ are equal. By counting the number of reset actions the input current is convertted into an frequency, were one count represents the average integrated charge in the period T. The relation between current and frequency is given by:

$$f = \frac{1}{I_{ref}\ \Delta T}\ I_{in} \tag{1}$$

The output frequency is not depending on the integration capacitor. However, it has to be selected carefully because it determines the amplitude of the integrator output voltage but also the sensitivity to noise and to the charge injection from the current switch. The relative error on the frequency depends only on the square root of the quadratic sum of the relative errors on the reference currents and on the reference time. Since the relative conversion error should be below 0.1 this could be reached without any calibration.

The output frequency of the CFC was measured over the whole dynamic range (see Fig.: 8) [4]. The measured frequency and the linearity error are shown in figure 8. The straight line is set equal to the data at 5 kHz. The CFC shows a deviation from the straight line of less than $\pm$ 0.5 % over an in-pute range of 500 pA to 100 μA. At low input currents, the error increases mainly because of the total leakage current. Above 100 μA, the one-shot works partly in the instable mode, which leads to a larger error. If the current exceeds 200 μA, the CFC is overloaded and becomes non-linear. The CFC

is well within the specified error margin of ± 10 %. The absolute error depends on the actual value of I_{ref} and T but is constant over the whole dynamic range.

CONCLUSION

Longitudinal beam loss distribution studies show that losses concentrate on locations with high β-functions (centre of quadrupole magnets) or where mechanical limitations of the aperture can be assumed. From shower simulations at the different loss locations we see that a set of six detectors around the quadrupoles is sufficient for localizing the beam losses and to distinct between the two beams. Ionization chambers will be used as shower particle detectors, which convert the particle loss rate into an electric current. The expected ionization chamber current, equivalent to the quench levels, varies between 500 pA and 500 μA depending on the different loss distributions and detector positions. Introducing a ten times higher sensitivity a dynamic range of 140 dB is needed. Several possibilities to measure the current of the chamber are discussed. The current-to-frequency converter is the most appropriate solution that is able to cover the wide dynamic range with low effort. It produces an output frequency proportional to the input current and simplifies the data transmission from the tunnel to the surface, where the beam loss signal is evaluated. Tests revealed an excellent linearity of the current to frequency converter. The frequency will be counted in intervalls of 40 μs and a serial word will be transmitted together with 5 other channel over the cable to the location of the threshold controller.

REFERENCES

1. J.B. Jeanneret et al., Quench levels and transient beam losses in LHC magnets, LHC Project Report 44, CERN, (1996).
2. A. Arauzo-Garcia et al., LHC Beam Loss Monitors, CERN-SL-2001-027-BI, CERN, (2001).
3. E. Gschwendtner et al., The Beam Loss Detection System of the LHC Ring, 8th European Particle Accelerator Conference, (2002).
4. W. Friesenbichler, Development of the Readout Electronics for the Beam Loss Monitors of the LHC, CERN-THESIS-2002-028 (2002).
5. H. Reeg and O. Keller, Linearer Strom-Frequenz-Konverter, Patent No. DE 195 20 315, Deutsches Patentamt, (1996).
6. H. Reeg, A Current Digitizer for Ionization Chambers, SEMS with high resolution and fast response, Proceedings of the 4 th Workshop on Diagnostics and Instrumentation in Particle Accelerators DIPAC, Daresbury, UK, pp. 140-142, (1999).
7. E. G. Shapiro, Linear Seven Decade Current-to-Frequency Converter, IEEE Trans. Nuclear Science, Vol. 17, pp. 335-344, (1970).